Supporting Information

Cancer Cell Specific Delivery of Photosystem I Through Integrin Targeted Liposome Shows Significant Anticancer Activity

Abhijit Saha,[1] Saswat Mohapatra,[2] Gaurav Das, [2] Batakrishna Jana,[1] Subhajit Ghosh,[1] Debmalya Bhunia,[1] Surajit Ghosh[*1,2]

1. Organic & Medicinal Chemistry Division, CSIR-Indian Institute of Chemical Biology, 4 Raja S. C. Mullick Road, Jadavpur, Kolkata-700032, West Bengal, India. Fax: +91-33-2473-5197/0284; Tel: +91-33-2499-5872

2. Academy of Scientific and Innovative Research (AcSIR), CSIR-Indian Institute of Chemical Biology Campus, 4 Raja S. C. Mullick Road, Kolkata 700 032, India.

* To whom Correspondence should be addressed: sghosh@iicb.res.in

Supplementary Figures

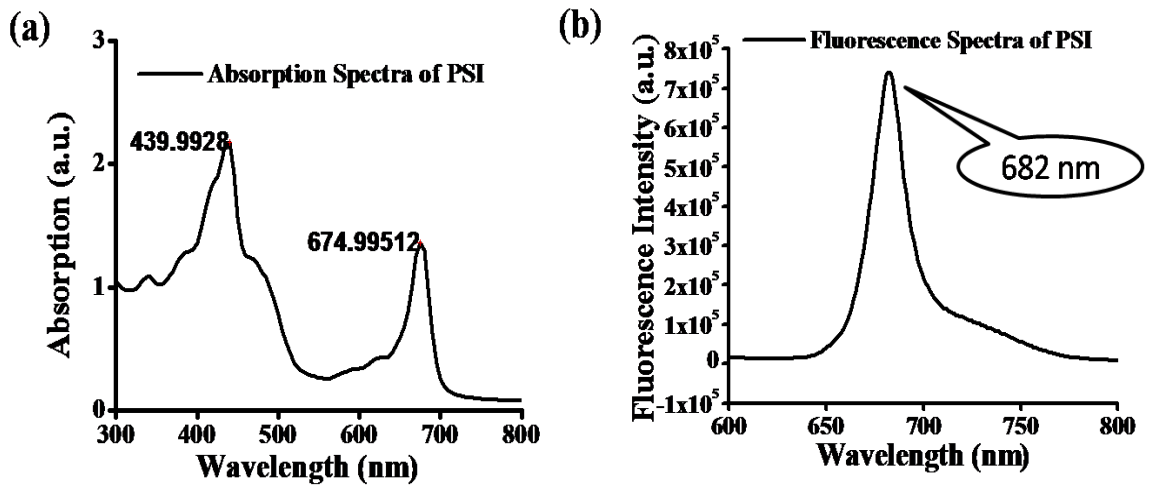

Figure S1: Characterization of PSI (a) Absorption spectra of PSI in water. (b) Fluorescence spectra of PSI in water.

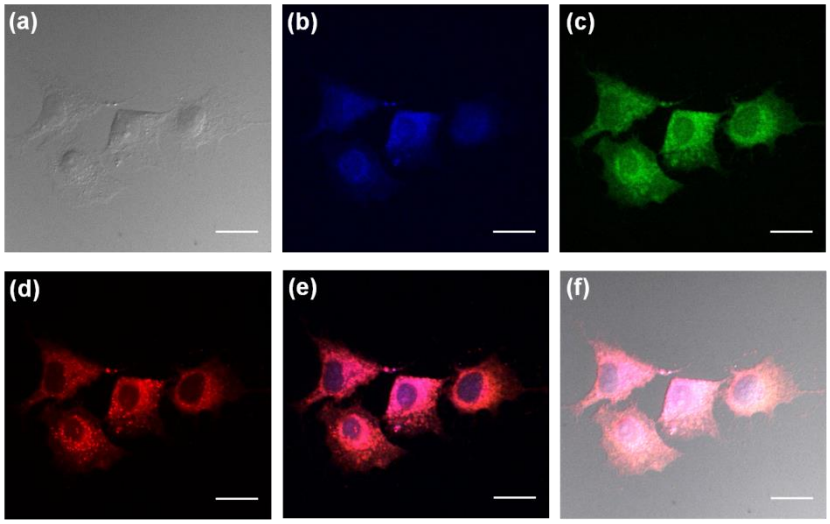

Figure S2: Cellular uptake of PSI in A549 cells in bright field (a), 405 nm channel (b), 488 nm channel (c), 561 nm channel (d), merged image of 405, 488, 561 nm channels (e) and merged image of bright field, 405, 488, 561 nm channels (f). Scale bars correspond to 20 μm.

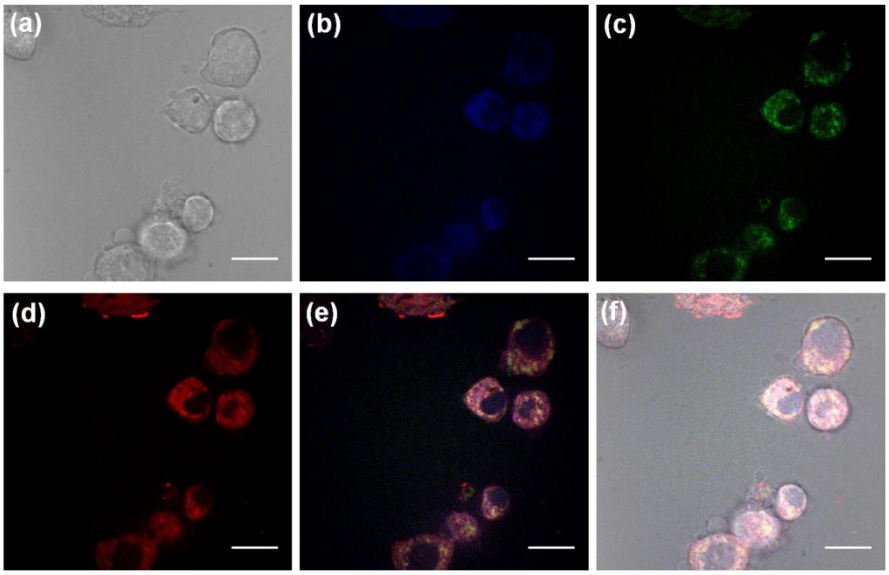

Figure S3: Cellular uptake of PSI in B16F10 cells in bright field (a), 405 nm channel (b), 488 nm channel (c), 561 nm channel (d), merged image of 405, 488, 561 nm channels (e) and merged image of bright field, 405, 488, 561 nm channels (f). Scale bars correspond to 20 μm.

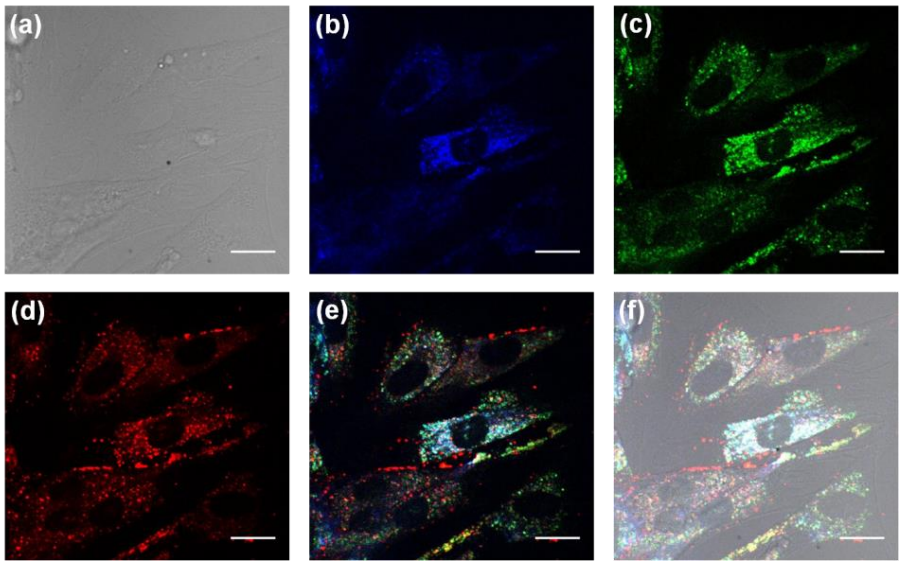

Figure S4: Cellular uptake of PSI in WI38 cells in bright field (a), 405 nm channel (b), 488 nm channel (c), 561 nm channel (d), merged image of 405, 488, 561 nm channels (e) and merged image of bright field, 405, 488, 561 nm channels (f). Scale bars correspond to 20 μm.

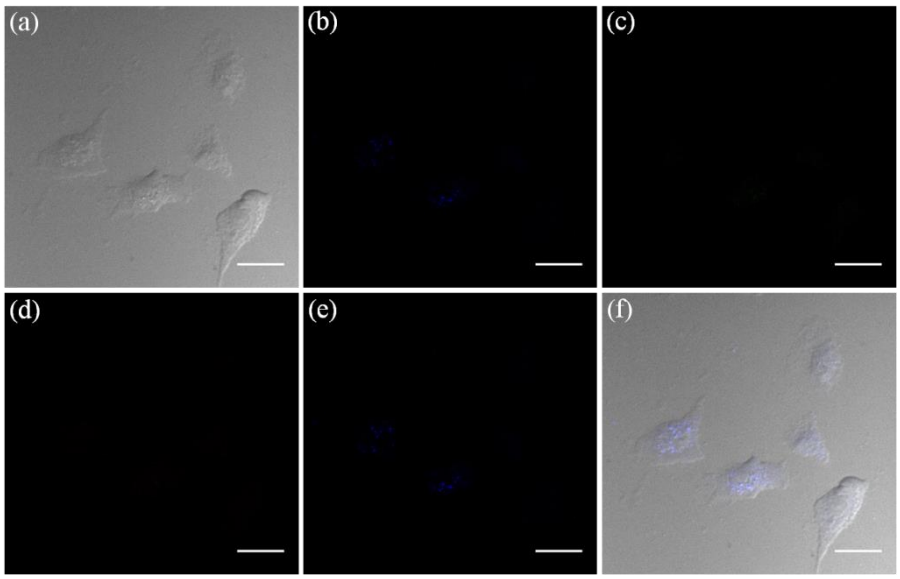

Figure S5: Images of control A549 cells (Cells are not treated with PSI) in bright field (a), 405 nm channel (b), 488 nm channel (c), 561 nm channel (d), merged image of 405, 488, 561 nm channels (e) and merged image of bright field, 405, 488, 561 nm channels (f). Scale bars correspond to 20 μm.

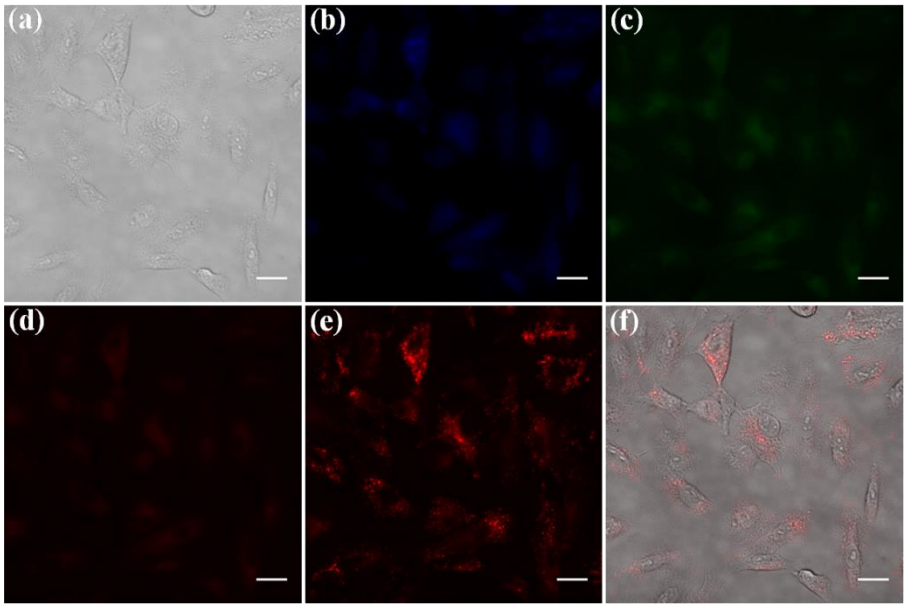

Figure S6: Images show cellular uptake of PSI into A549 cells in bright field (a), DAPI channel (b), FITC channel (c), TRITC channel (d), Cy5 channel (e) and merged channels (f). Scale bars correspond to 20 μm.

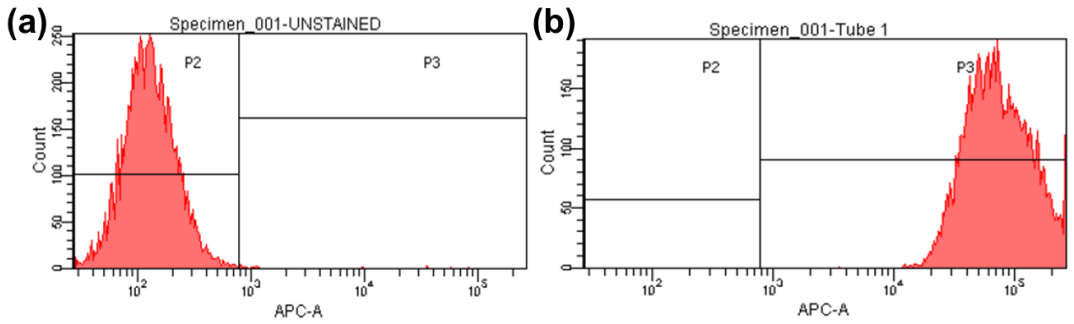

	P2 (%)	P3 (%)
CONTROL	99.5	0.2
PS1	0	100

Figure S7: Cellular uptake of PSI into A549 cells was studied using FACS. (a) Cells were not treated with PSI (control cells). (b) Cells were treated with PSI.

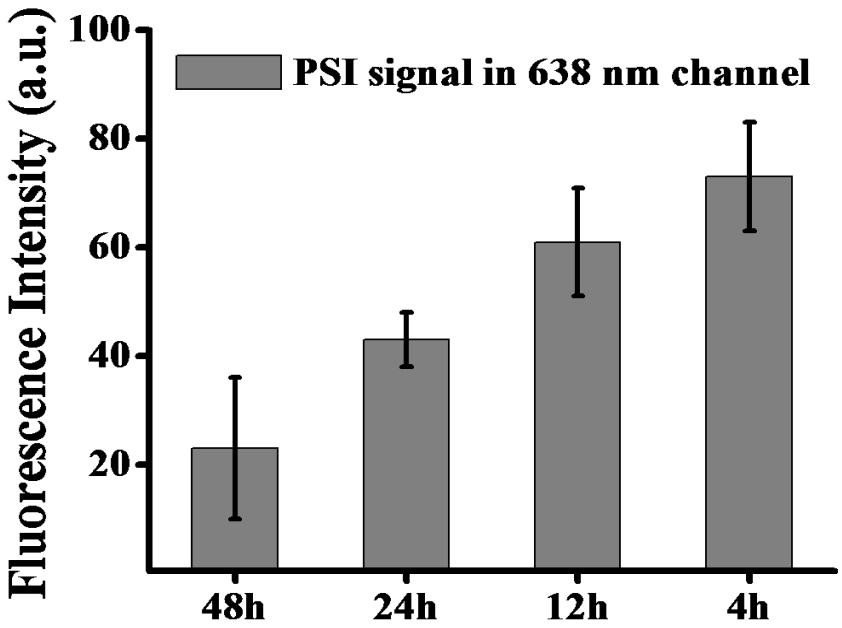

Figure S8: Degradation of PSI with time inside the cell. Fluorescence signal of the images taken in 638 nm channel was measured using Image-J software.

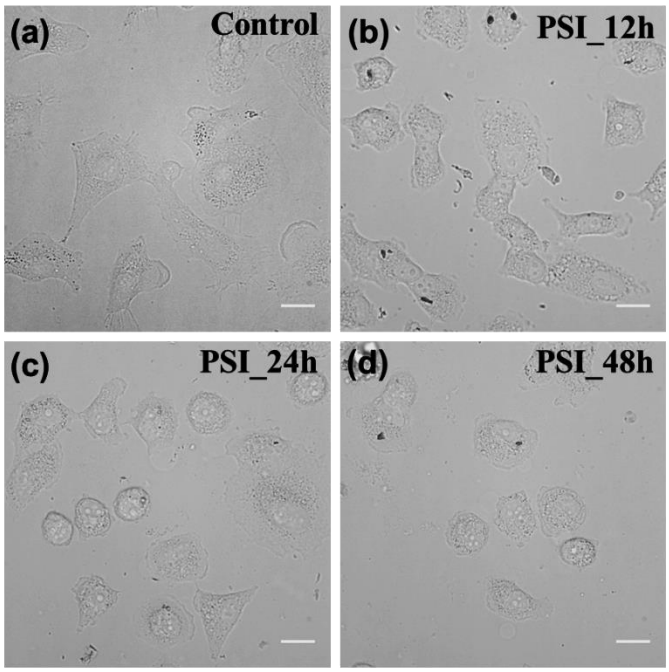

Figure S9: Effect of PSI on the cellular morphology of A549 cell with time. Scale bars correspond to 20 µm.

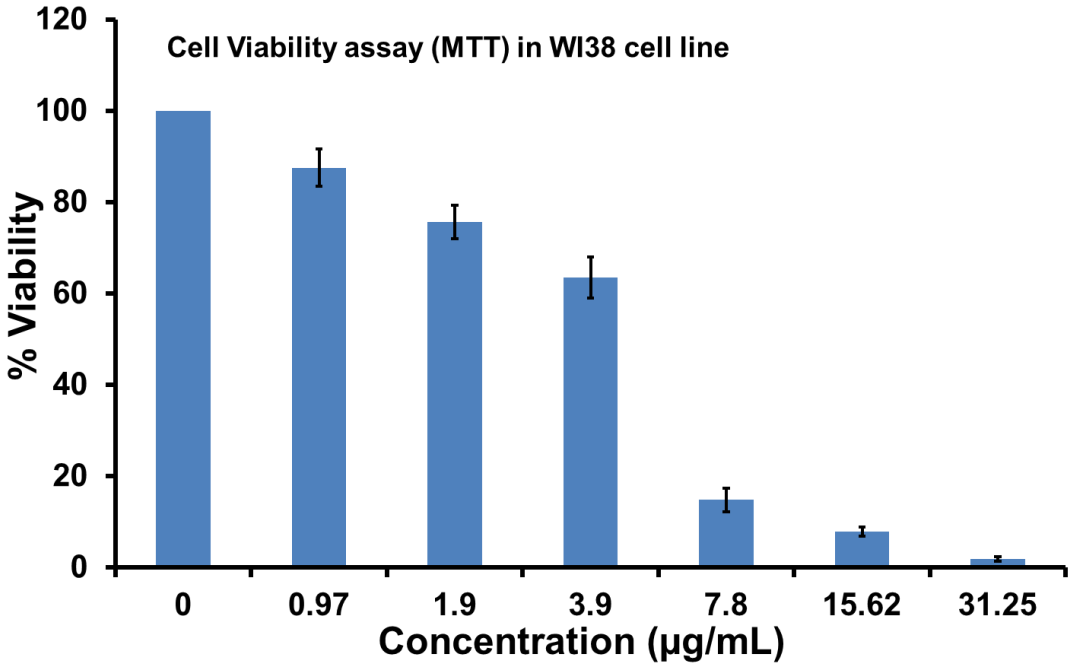

Figure S10: Effect of PSI on the cellular viability of WI38 normal cell.

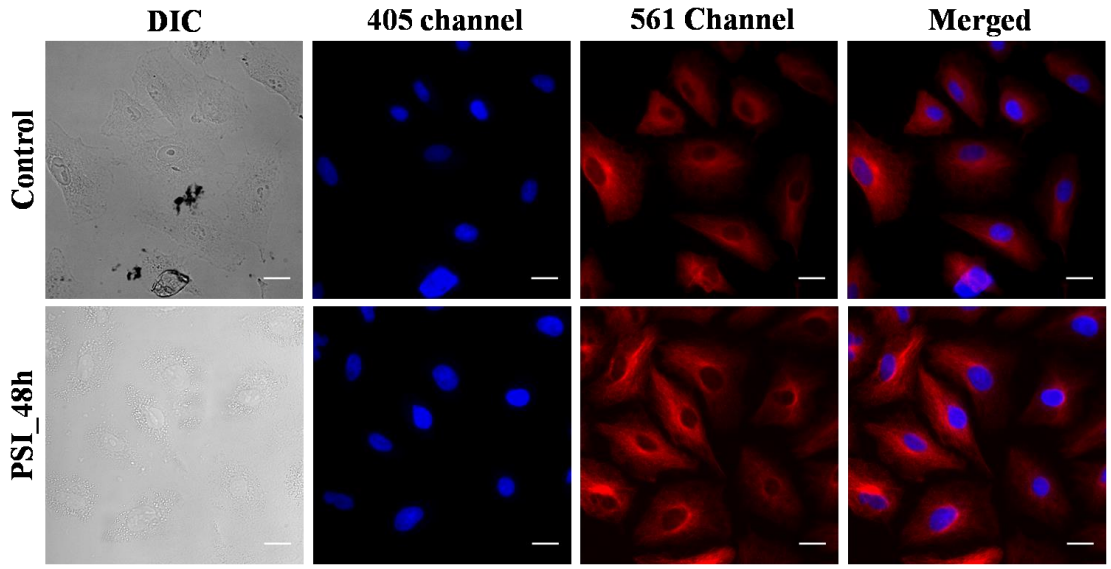

Figure S11: Images show that PSI has no effect on the microtubule network of the A549 cells. Scale bars correspond to 20 μm.

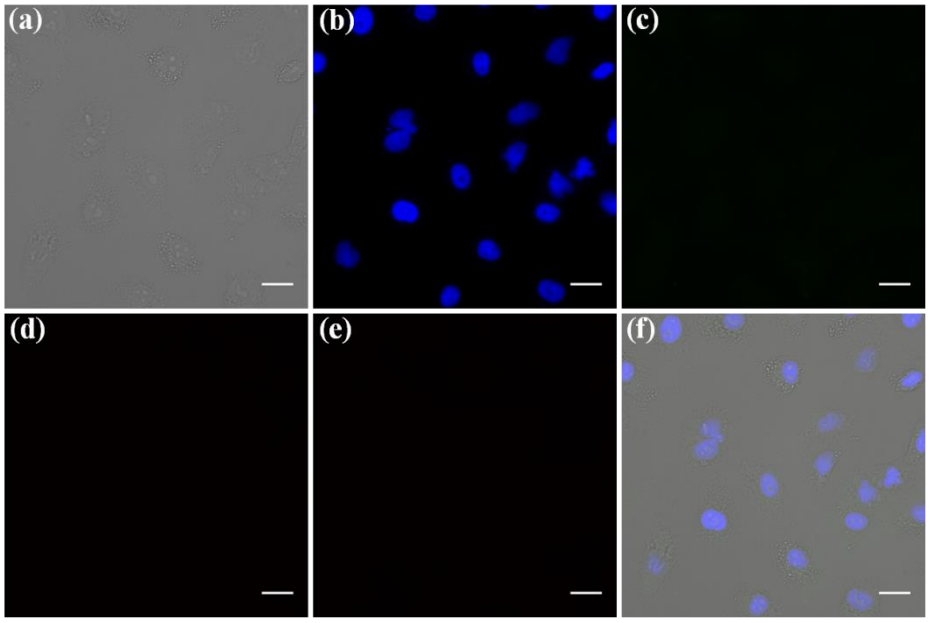

Figure S12: Images of control A549 cells for BubR1 activation in bright field (a), 405 nm channel (b), 488 nm channel (c), 561 nm channel (d), 638 nm channel (e) and merged image (f). Scale bars correspond to 20 μm.

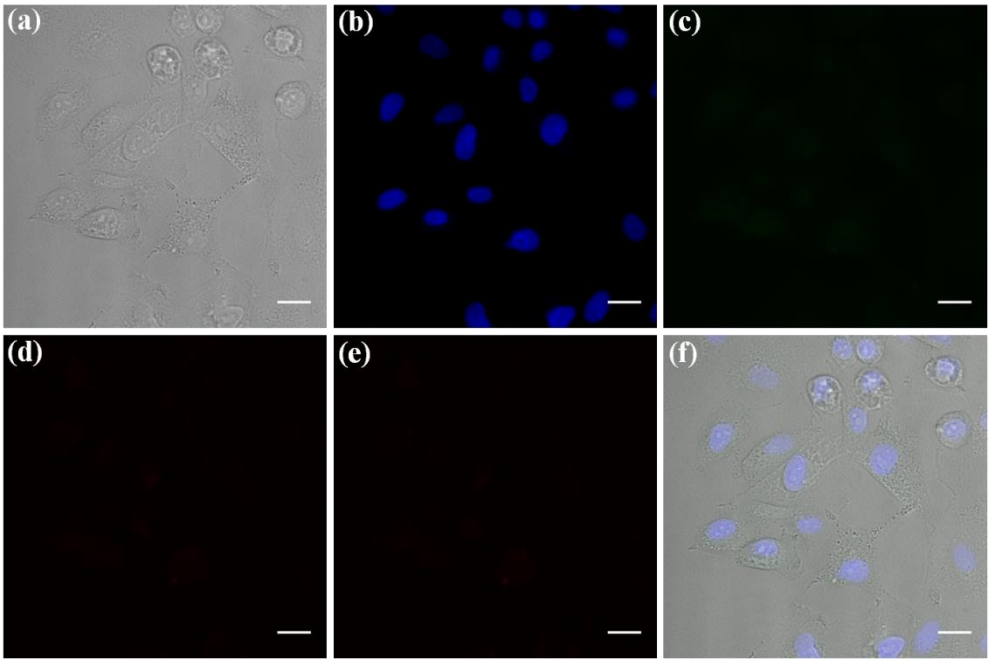

Figure S13: Images of A549 cells after treatment with PSI for BubR1 activation in bright field (a), 405 nm channel (b), 488 nm channel (c), 561 nm channel (d), 638 nm channel (e) and merged image (f). Scale bars correspond to 20 μm.

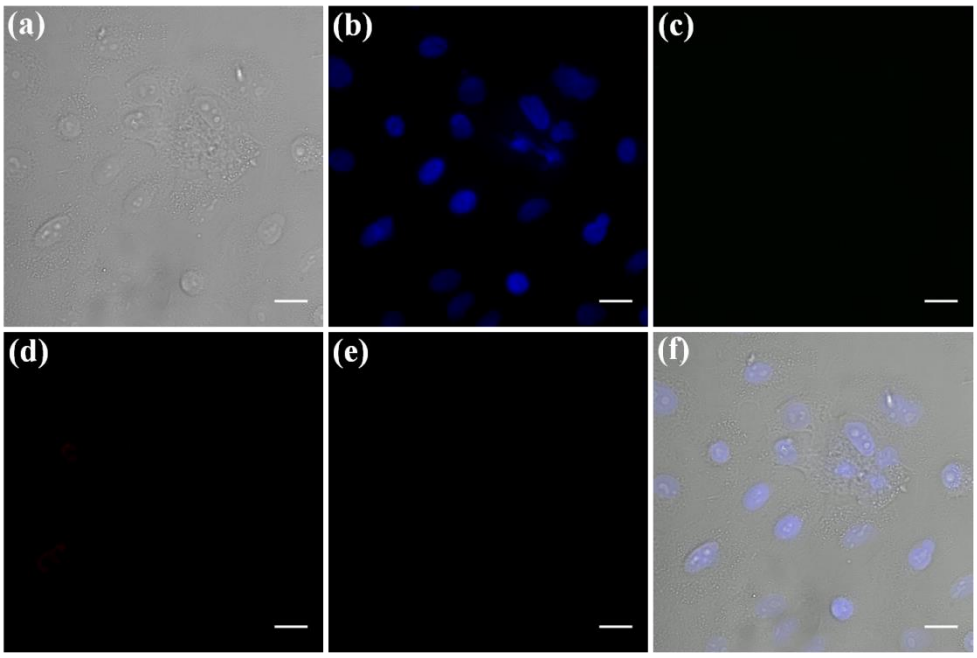

Figure S14: Images of control A549 cells for Mad2 activation in bright field (a), 405 nm channel (b), 488 nm channel (c), 561 nm channel (d), 638 nm channel (e) and merged image (f). Scale bars correspond to 20 μm.

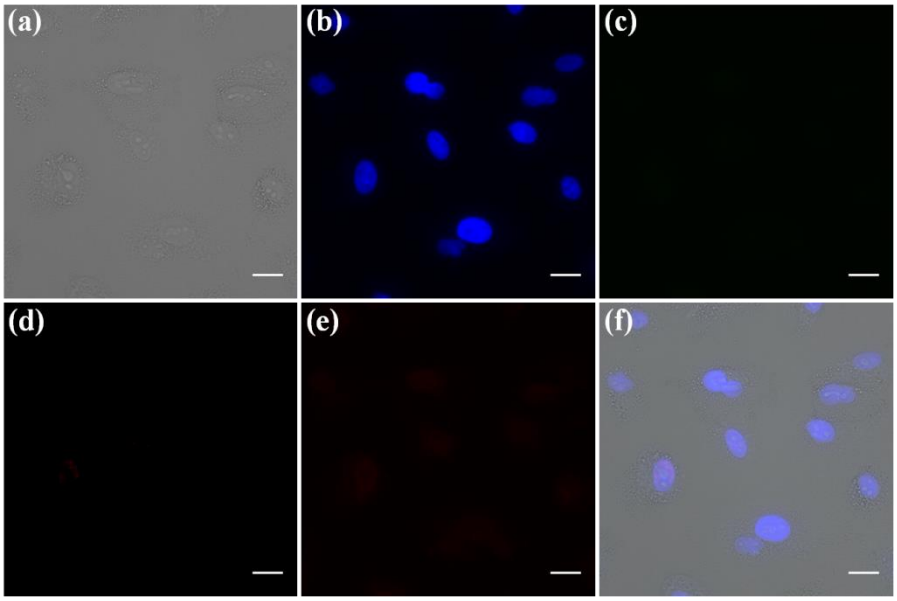

Figure S15: Images of A549 cells after treatment with PSI for Mad2 activation in bright field (a), 405 nm channel (b), 488 nm channel (c), 561 nm channel (d), 638 nm channel (e) and merged image (f). Scale bars correspond to 20 μm.

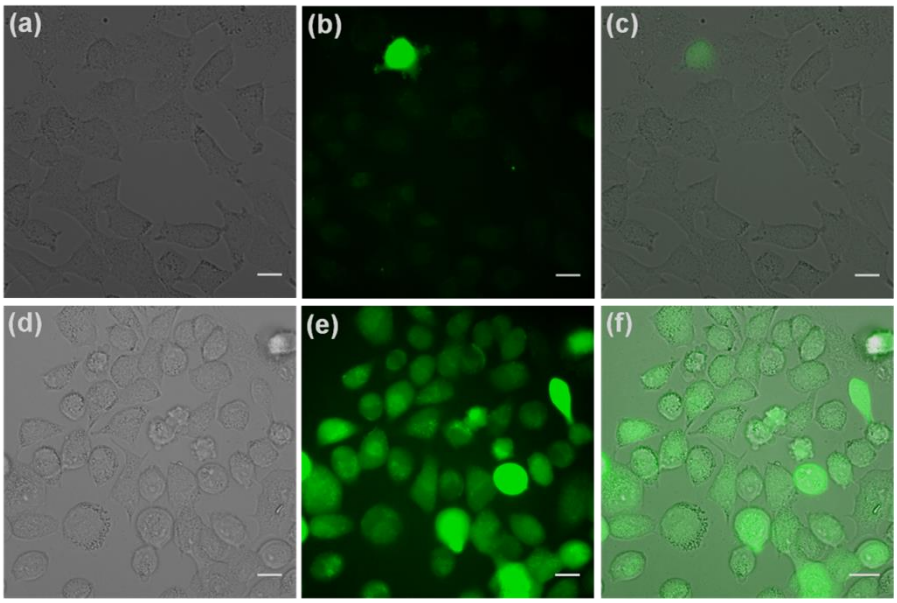

Figure S16: Generation of reactive oxygen species in A549 cells after treatment with PSI (according to DCF method). Images of control A549 cells (cells were not treated with PSI) in bright field (a), 488 nm channel (b) and merged image (c).Images of A549 cells (treated with PSI) in bright field (d), 488 nm channel (e) and merged image (f). Scale bars correspond to 20 μm.

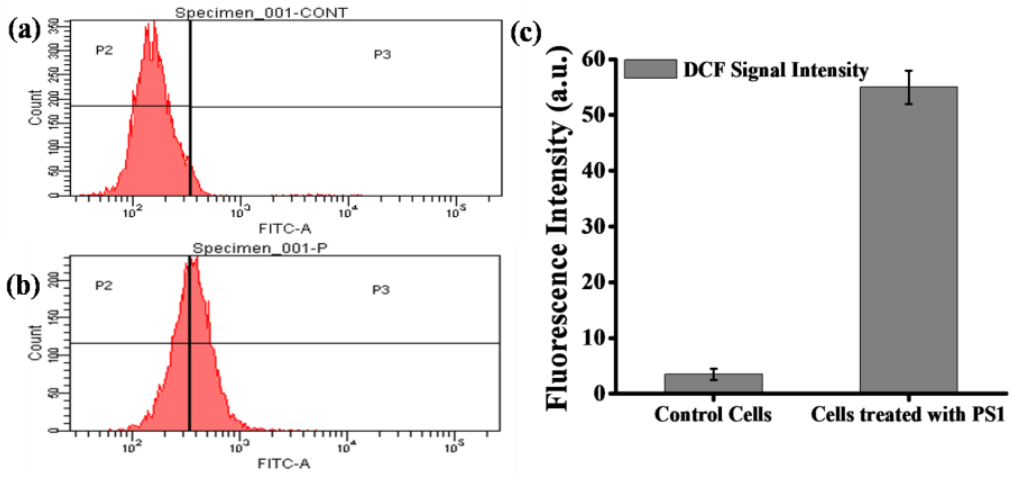

Figure S17: Generation of reactive oxygen species in A549 cells after treatment with PS1 was studied using FACS. (a) Cells were not treated with PSI (control cells). (b) Cells were treated with PSI. (c) Quantitative bar diagram shows greater FITC signal in cells which were treated with PSI.

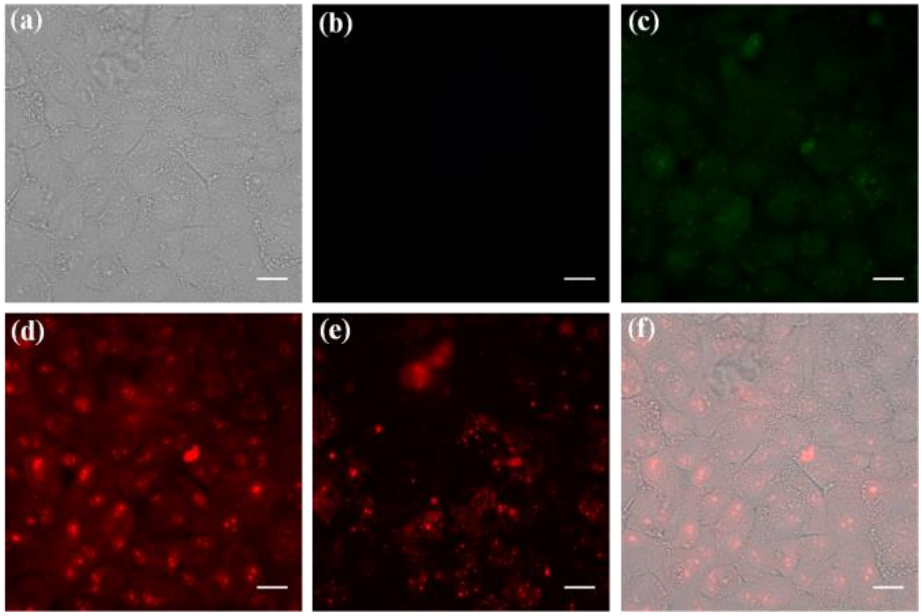

Figure S18: Images showing the generation of reactive oxygen species (according to DHE method) in A549 cells after treatment with PSI in bright field (a), 405 nm channel (b),488 nm channel (c), 561 nm channel (d), 638 nm channel (e) and merged image (f). Scale bars correspond to 20 μm.

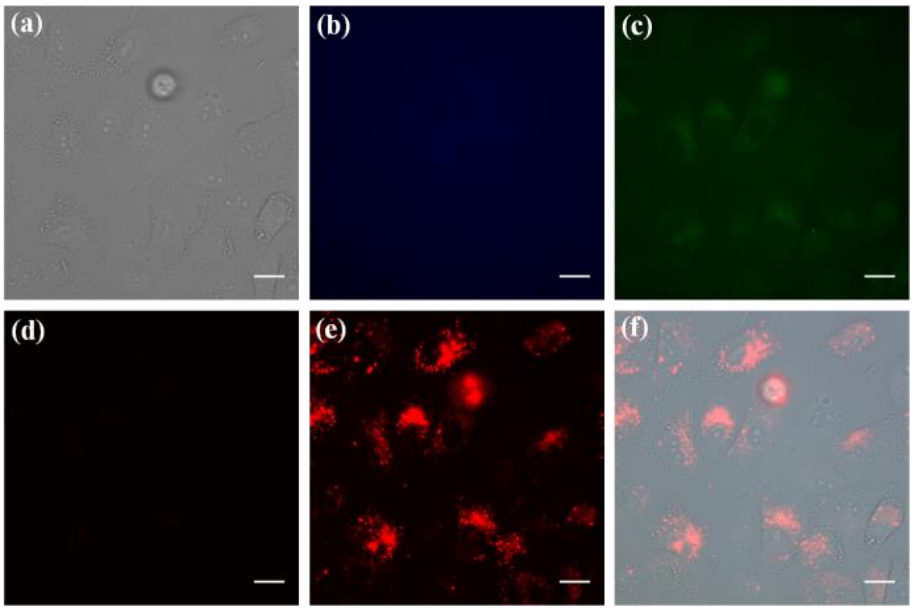

Figure S19: Images showing the signal of PSI in A549 cells (PSI control) in bright field (a), 405 nm channel (b), 488 nm channel (c), 561 nm channel (d), 638 nm channel (e) and merged image (f). Scale bars correspond to 20 μm.

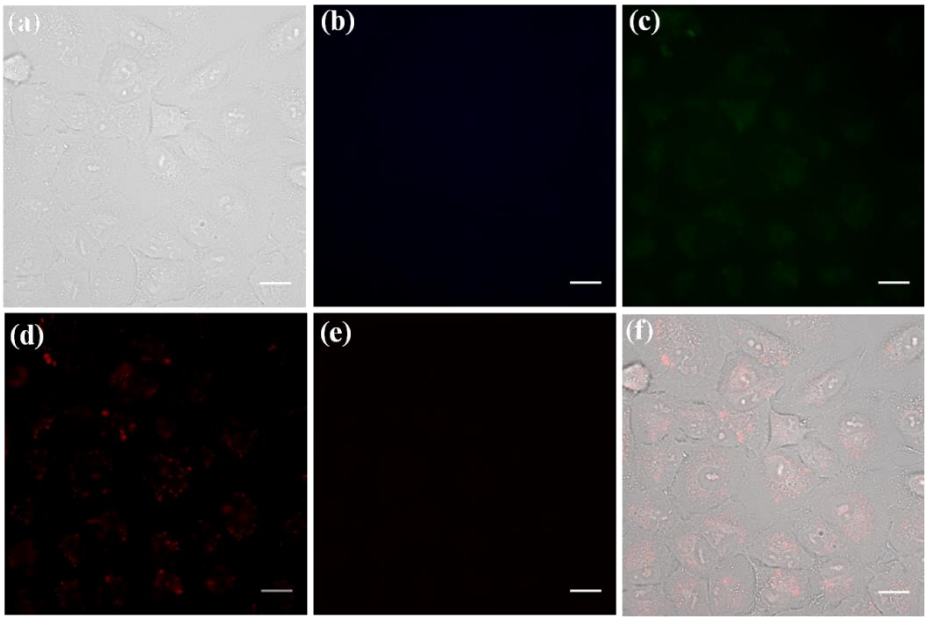

Figure S20: Images showing the generation of reactive oxygen species (according to DHE method) in control A549 cells (cells were not treated with PSI) in bright field (a), 405 nm channel (b),488 nm channel (c), 561 nm channel (d), 638 nm channel (e) and merged image (f). Scale bars correspond to 20 μm.

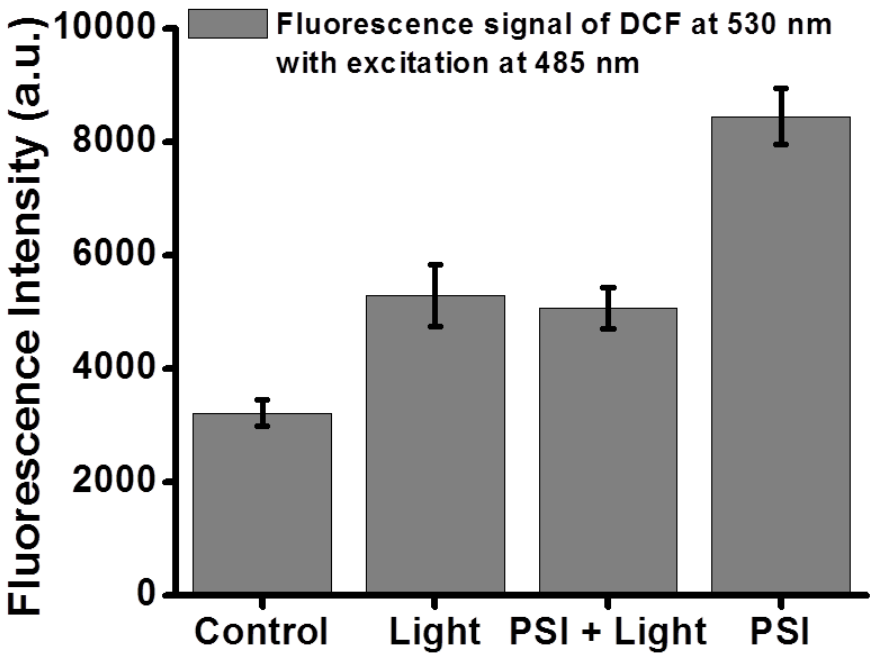

Figure S21: Generation of reactive oxygen species in A549 cells after treatment with PSI (according to DCF method). Cells, not treated with PSI and light irradiation, were regarded as control.

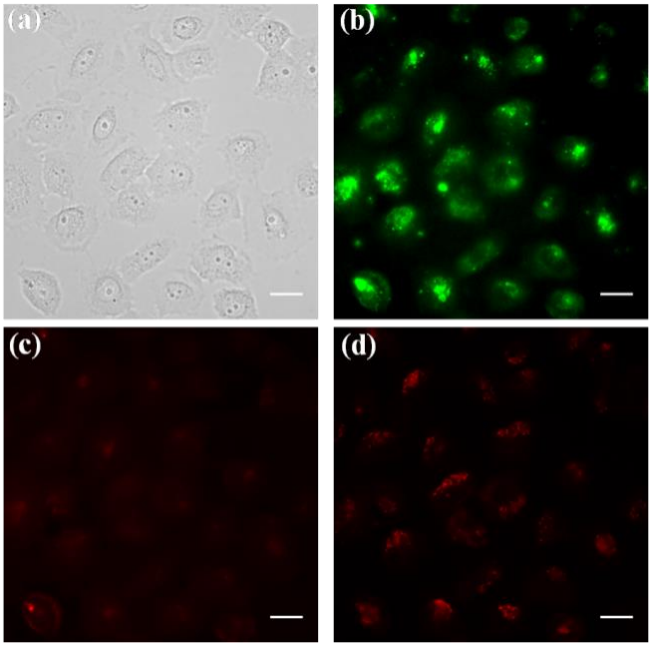

Figure S22: Fluorescence images of annexin V and propidium iodide assay in A549 cells after treatment with PSI in bright field (a), 488 nm channel (b), 561 nm channel (c) and 638 nm channel (d). Scale bars correspond to 20 μm.

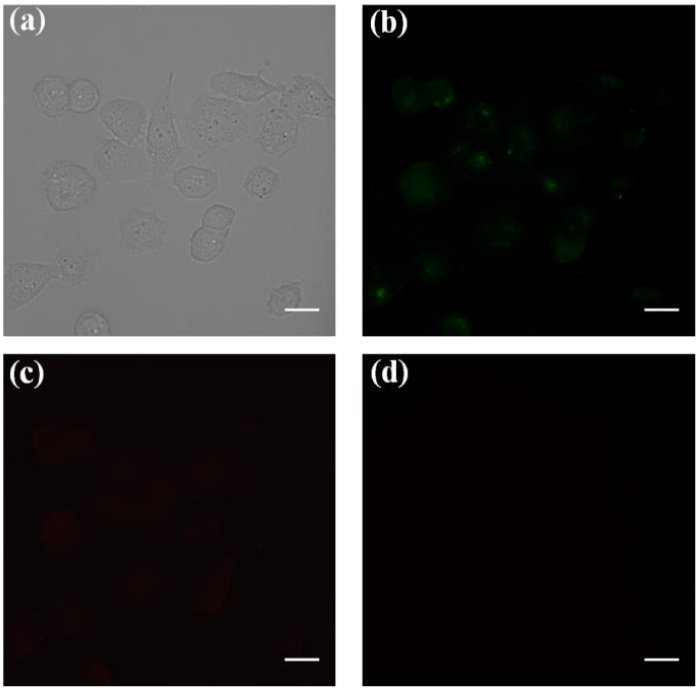

Figure S23: Fluorescence images of annexin V and propidium iodide assay in control A549 (cells were not treated with PSI) in bright field (a), 488 nm channel (b), 561 nm channel (c) and 638 nm channel (d). Scale bars correspond to 20 μm.

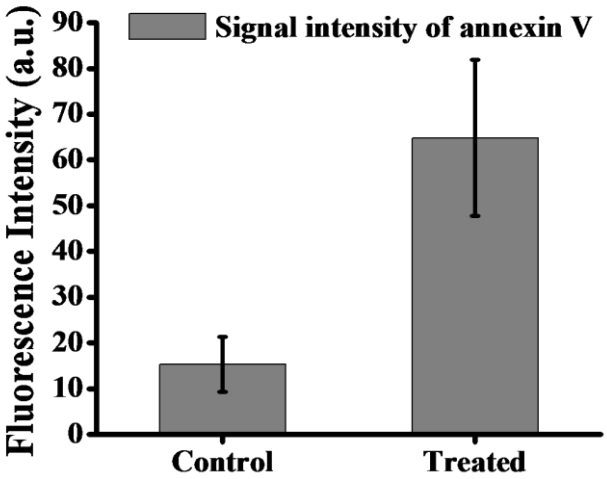

Figure S24: Increase of fluorescence intensity of annexin V in A549 cells after treatment with PSI compared to control A549 cells (cells were not treated with PSI).

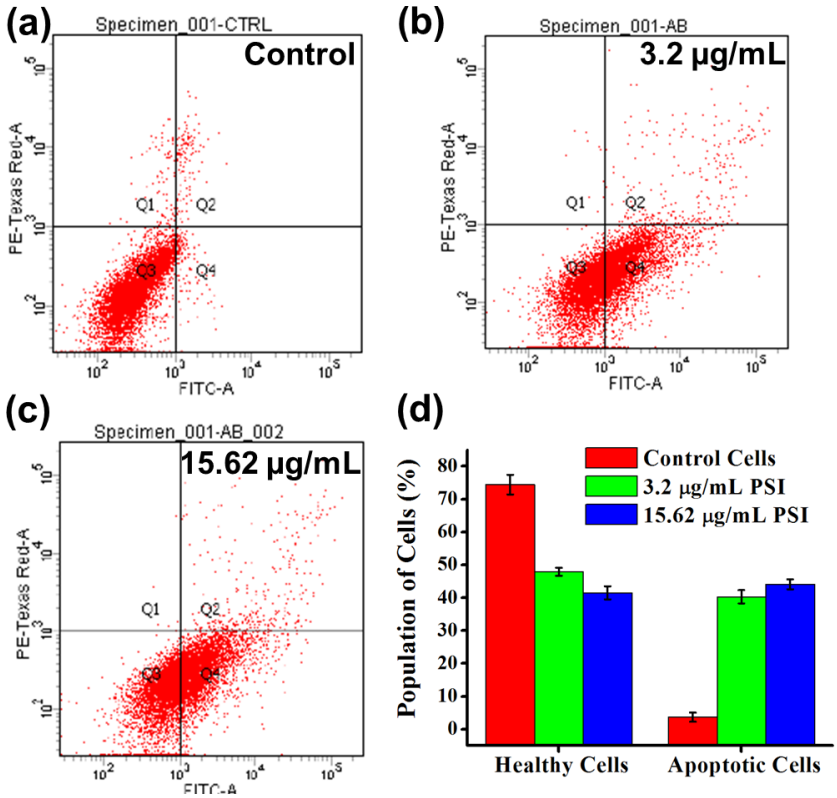

Figure S25: Apoptotic death of B16F10 cells after treatment with PSI. (a) Control B16F10 cells. (b) Cells were treated with 3.2 µg/mL solution of PSI. (c) Cells were treated with 15.62 µg/mL solution of PSI. (d) Comparative bar diagram shows apoptotic death of cells increases with increasing the concentration of PSI.

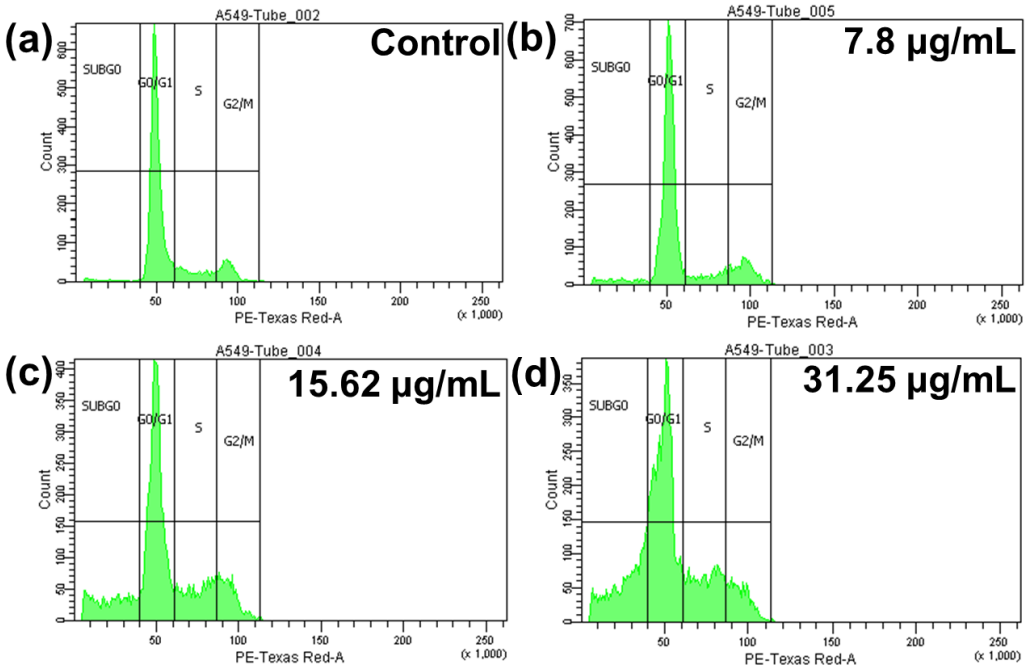

Figure S26: Study of cell cycle of A549 cells after treatment with PSI. (a) Control A549 cells. (b) Cells were treated with 7.8 µg/mL solution of PSI. (c) Cells were treated with 15.62 µg/mL solution of PSI. (d) Cells were treated with 31.25 µg/mL solution of PSI.

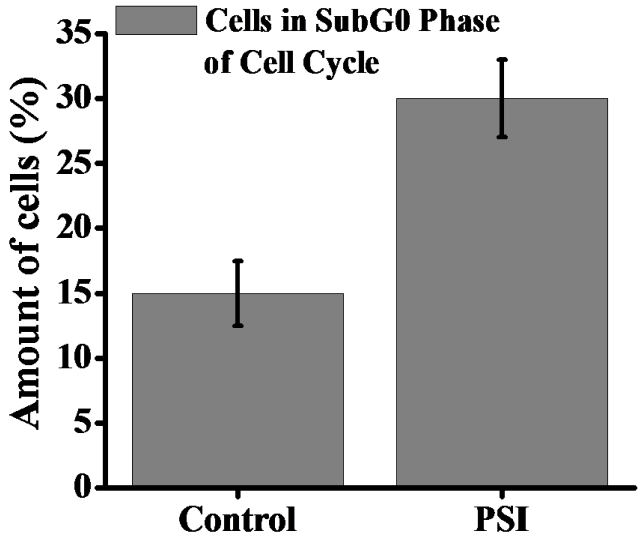

Figure S27: Cell cycle study of B16F10 cells after treatment with 15.62 µg/mL solution of PSI. Comparative bar diagram shows that amount of SubG0 phase of cell cycle was increased after PSI treatment.

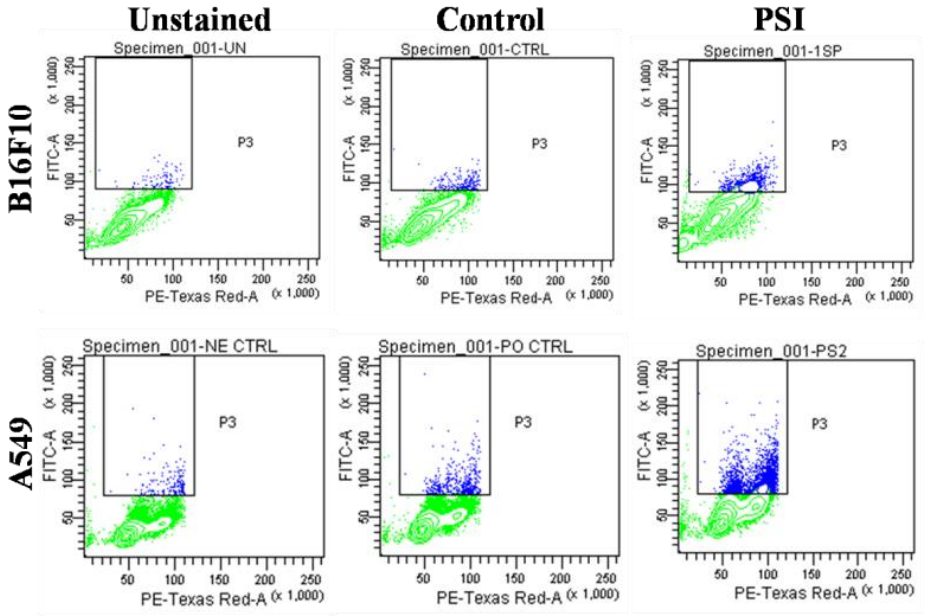

Figure S28: Images of TUNEL assay show the increase of the amount of fragmented DNA in B16F10 and A549 cells after treatment of PSI.

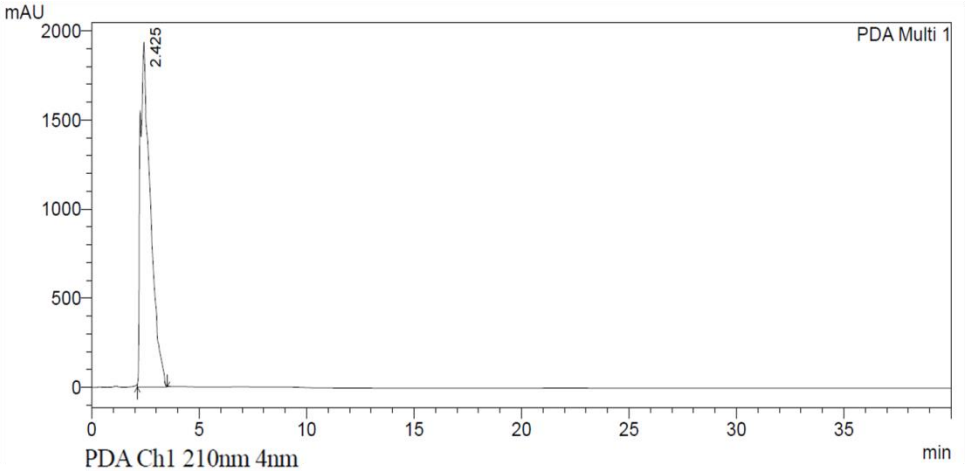

Peak#	Ret. Time	Area	Height	Area %	Height %
1	2.425	63195427	1934217	100.000	100.000
Total		63195427	1934217	100.000	100.000

Figure S29: Analytical HPLC chromatogram of the long chain attached LDV lipopeptide.

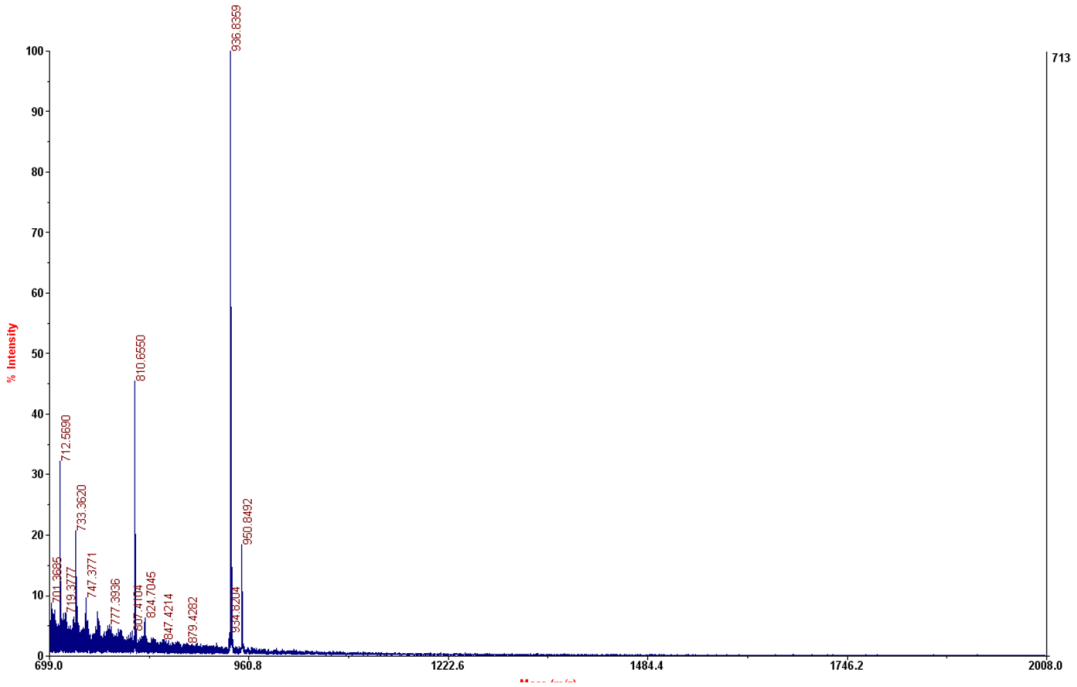

Figure S30: MALDI mass spectra of the LDV long chain lipopeptide (m/z =936.9).

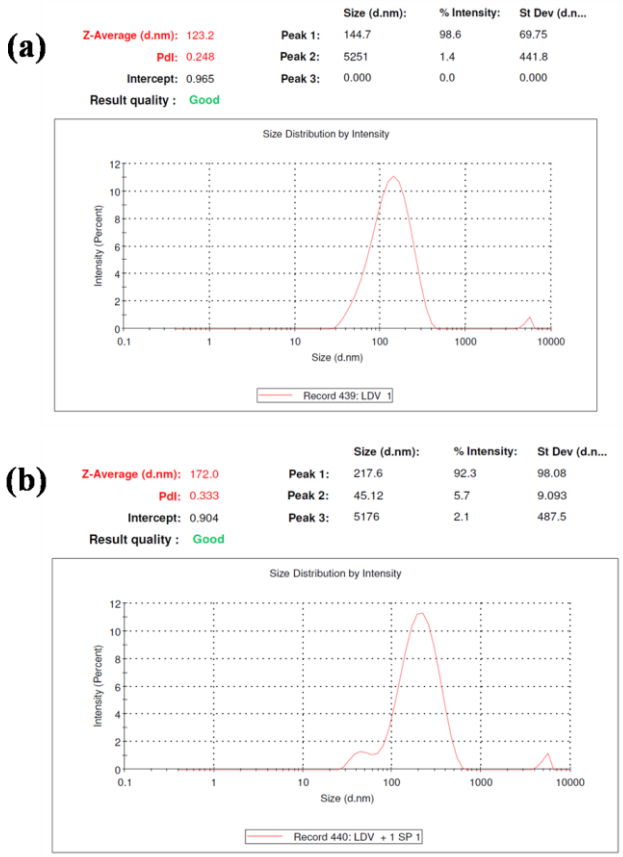

Figure S31: Dynamic light scattering (DLS) study to measure the size of (a) LDV-liposome (123.2 nm) and (b) LDV-liposome-PSI (172 nm).

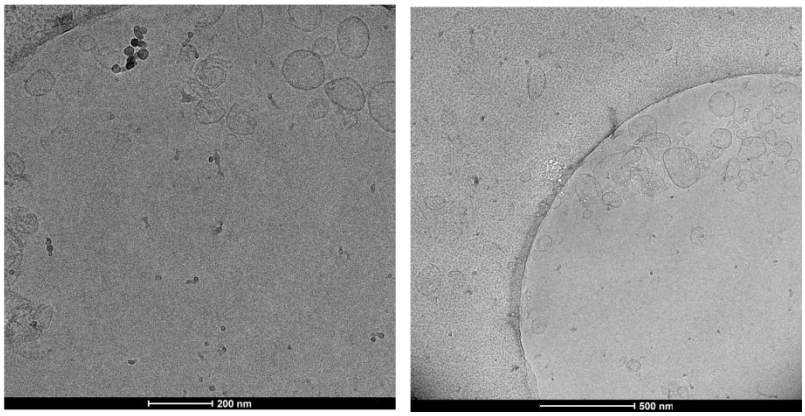

Figure S32: Cryo Transmission electron microscopy of the LDV liposome-PSI.

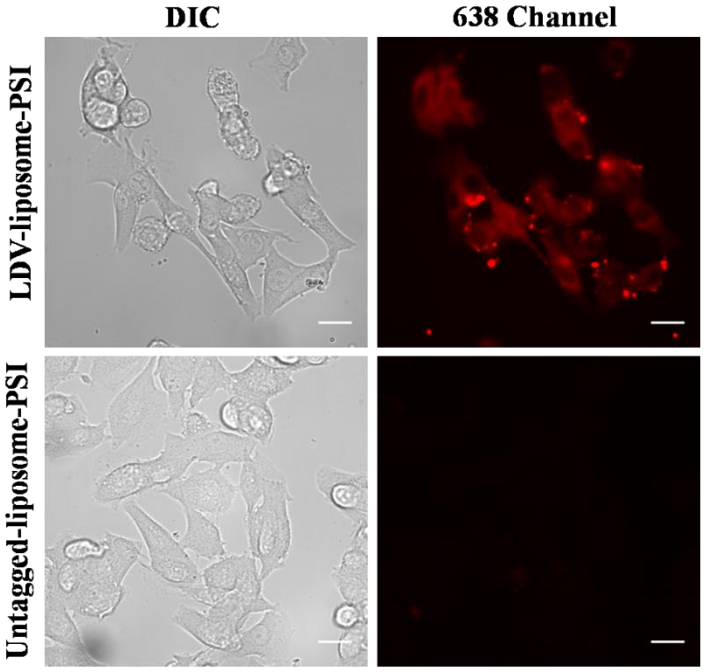

Figure S33: Comparative cellular uptake of LDV-liposome-PSI and untagged-liposome-PSI into B16F10 cells in 2h. Scale bars correspond to 20 μm.

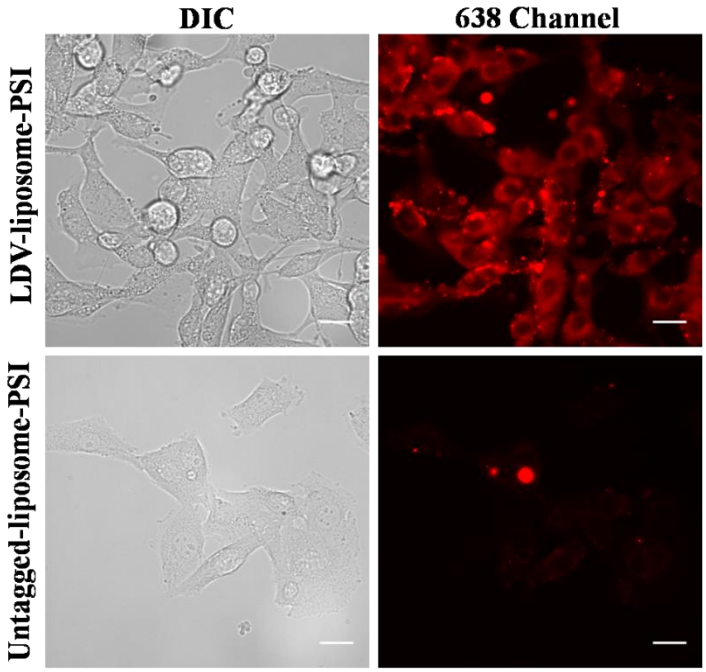

Figure S34: Comparative cellular uptake of LDV-liposome-PSI and untagged-liposome-PSI into B16F10 cells in 4h. Scale bars correspond to 20 μm.

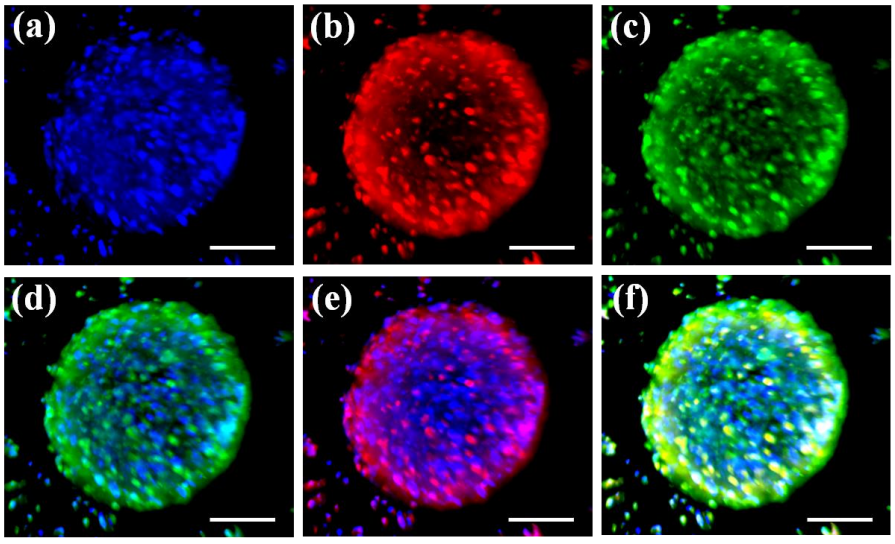

Figure S35: Cellular uptake of PSI in tumor spheroid at 405 nm channel (a), 561 nm channel (b), 488 nm channel (c), merged image of 405, 488 nm channels (d), merged image of 405, 561 nm channels (e) and merged image of 405, 488, 561 nm channels (f). Scale bars correspond to 100μm.

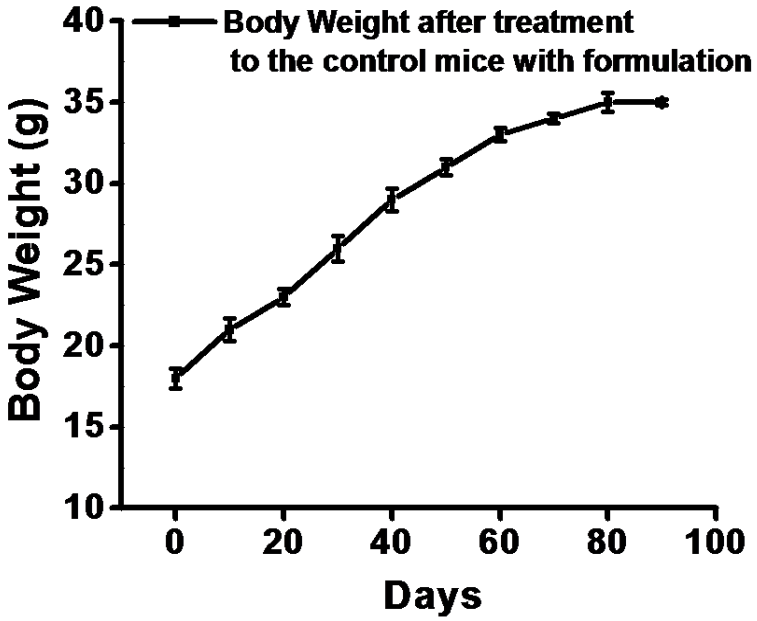

Figure S36: Body weight of C57BL/6J mice was observed upto 90 days along with treatment with LDV liposomal PSI.

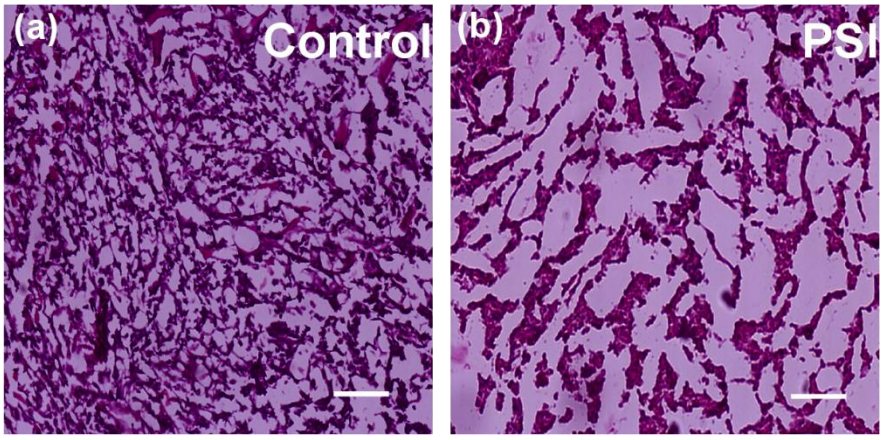

Figure S37: Melanoma tumor slices from C57BL/6J mice were stained with hematoxylin and eosin (HE). (a) Tumor slice of control mice and (b) tumor slice of treated mice were imaged after staining under 10X objective. Scale bars correspond to 100 µm.